Evidence of the Differential Biotransformation and Genotoxicity of ZnO and CeO2 Nanoparticles on Soybean (Glycine max) Plants

ARTICLE *in* ENVIRONMENTAL SCIENCE & TECHNOLOGY · APRIL 2010

Impact Factor: 5.33 · DOI: 10.1021/es903891g · Source: PubMed

Published in final edited form as:
Environ Sci Technol. 2010 October 1; 44(19): 7315–7320. doi:10.1021/es903891g.

Evidence of the differential biotransformation and genotoxicity of ZnO and CeO_2 nanoparticles on soybean (*Glycine max*) plants

Martha L. López-Moreno[†,£], **Guadalupe de la Rosa**[†,‡], **José Á. Hernández-Viezcas**[†], **Hiram Castillo-Michel**[§], **Cristian E. Botez**[‡‡], **José R. Peralta-Videa**[†], and **Jorge L. Gardea-Torresdey**[†,§]

[†]Chemistry Department, The University of Texas at El Paso, 500 W. University Ave., El Paso, TX. 79968

[‡‡]Physics Department, The University of Texas at El Paso, 500 W. University Ave., El Paso, TX. 79968

[§]Environmental Sciences and Engineering Ph.D. Program, The University of Texas at El Paso, 500 W. University Ave., El Paso, TX. 79968

[‡]Departamento de Ingeniería Química, Universidad de Guanajuato. Col. N. Alta s/n, Guanajuato, Gto., 36050

[£]Department of Chemistry, University of Puerto Rico at Mayaguez, Mayaguez, PR 00681

Abstract

Concern and interest related to the effects of nanomaterials on living organisms are growing in both the scientific and public communities. Reports have described the toxicity of nanoparticles (NPs) on micro and macro organisms, including some plant species. Nevertheless, to the authors' knowledge there are no reports on the biotransformation of NPs by edible terrestrial plants. Here, shown for the first time, is evidence pertaining to the biotransformation of ZnO and CeO_2 NPs in plant seedlings. Although the NPs did not affect soybean germination, they produced a differential effect on plant growth and element uptake. By using synchrotron X-ray absorption spectroscopy we obtained clear evidence of the presence of CeO_2 NPs in roots, whereas ZnO NPs were not present. Random amplified polymorphic DNA assay was applied to detect DNA damage and mutations caused by NPs. Results obtained from the exposure of soybean plants to CeO_2 NPs show the appearance of four new bands at 2000 mg L^{-1} and three new bands at 4000 mg L^{-1} treatment. In this study we demonstrated genotoxic effects from the exposure of soybean plants to CeO_2 NPs.

Keywords

ZnO; CeO_2; Nanoparticles; Nanotoxicity; Genotoxicity; XAS

Introduction

Nanotechnology has emerged as an innovative technology for the elaboration and use of new nanomaterials (NMs) in industry and many fields of research (1). The wide range of NM application represents a challenge for researchers and government agencies, alike, who deal not only with scarce information about the fate and transport of NMs in the environment, but also with uncertainties about probable health hazards to living organisms (2,3). Of particular

*Corresponding author: jgardea@utep.edu (J. Gardea-Torresdey, Phone (915) 747-5359; Fax (915) 747-5748).

importance is the knowledge related to the plant response to NM impacts, due mainly to their role of preserving environmental equilibrium as well as their importance as a food source.

Defense mechanisms activated in biological organisms under stress are analyzed through different analytical techniques. For instance, reduction and complexation of toxic ionic forms are known as types of attenuation for heavy metal stress. This sort of element modification is studied by using X-ray absorption spectroscopy (XAS), which gives information about speciation and coordination environment of metals within tissues (4). Heavy metal toxicity can also be detected by analyzing DNA alterations by molecular biology techniques such as the random amplified polymorphic DNA (RAPD) (5). Through this technique, random segments of genomic DNA are amplified by different primers of a nucleotide sequence. These primers create new amplicons of different lengths which are separated by gel electrophoresis obtaining the DNA fingerprint (6).

Soybean (*Glycine max*) is one of the major crops grown worldwide for human consumption. This plant is also an important precursor in the elaboration of several biomaterials and biodiesel (7). Because of its high biomass production and easy cultivation, soybean has been studied as a potential metal accumulator (8,9).

The absorption of metals by plants depends on several factors, including the element's availability and uptake, and the storage capacity of plants (8). Soybean has shown physiological responses to different sources of nutritional elements. Bernal et al. (10) studied the effects of Cu on Zn and Fe uptake, as well as photosynthetic activity of soybean leaves. These researchers reported that soybean plants showed different signs of toxicity depending on the source of Cu. Engineered NMs may be a potential source for metal release that can eventually be made available for uptake by biological systems (11). In addition, to the authors' knowledge, there is no information about the speciation and biotransformation of these nanomaterials within soybean tissues.

The aims of this study were to determine the biotransformation of ZnO and CeO_2 nanoparticles (NPs) on soybean plants, their impact on DNA stability, and the effects on germination and seedling growth. Data about metal concentration and oxidation state in tissues were obtained using inductively coupled plasma-optical emission spectroscopy (ICP-OES) and X-ray absorption spectroscopy (XAS), respectively. DNA isolation was performed using the Wizard™ Genomic DNA extraction kit (Promega A1120). DNA yield was determined using the Nanodrop spectrophotometer for quantification of double stranded DNA. Results from this research will contribute to the enrichment of knowledge pertaining to the interactions of some nanomaterials with living plants.

Methodology

NP characterization

ZnO and CeO_2 NPs were purchased from Meliorum Technologies (Rochester, NY). X-ray diffraction (XRD) analysis showed an impurity phase in the ZnO NPs (Figure 1 Supporting information, SI). The average particle size was determined from the full width at half the maximum (FWHM) of the (110) Bragg peak using the Scherrer equation (12). The FWHM was obtained from the best fit of the peak profile to a combination of Gaussian and Lorentzian functions. Particle size and composition of NPs were determined on a Siemens D500 X-ray diffractometer (New York, NY, USA) equipped with a Braun position-sensitive detector. The samples were weighted and loaded in a flat-plate sample holder. Powder XRD patterns were collected in the reflectivity geometry within the 20°–60° 2θ-range (λ=1.5406Å). For the ICP-OES characterization, 100 mg of NPs were digested in a microwave oven using a mixture of

plasma pure HNO_3 + H_2O_2 (1:4) for CeO_2 after Packer et al. (13) and 3 mL of plasma pure HNO_3 for ZnO NPs.

Preparation of ZnO and CeO_2 suspensions

Suspensions of ZnO and CeO_2 NPs were prepared at 0 (control), 500, 1000, 2000, and 4000 mg L^{-1} using Millipore water (MPW). To avoid aggregation, the NP suspensions were sonicated for 30 min after Lin and Xing (6), and the pH of each suspension was recorded. pH of Hoagland's solution was adjusted to 5.8 ± 0.1 with NaOH 0.1 M. Solution pH after NP addition was in the range of 6.5 to 7.0 ± 0.1. No further pH adjustments were performed to avoid additional sources of variation in solutions. Further studies need to be done in order to determine the effects of pH and sonication on possible NP agglomeration.

Germination experiments

Soybean (*Glycine max*) seeds were purchased from Howe Seeds (Mclaughlin, SD). Seeds were treated for 30 min with a 4% NaClO solution for disinfection, followed by rinsing with sterilized MPW. Germination paper (Nasco, Fort Atkinson, WI) cut to fit regular Petri dishes was used as inert material. A piece of paper was placed in the Petri dish and 5 mL of ZnO or CeO_2 NP suspensions, at the appropriate concentrations, were added (6). Triplicate samples of thirty seeds were placed in every Petri dish, covered by another piece of paper followed by 10 drops of antibiotic-antimycotic solution (A5955, Sigma, St Louis, MO). Finally, the dishes were covered with aluminum paper (to allow seed germination in a dark environment) and set on lab benches at room temperature (25°C)".

The germination was recorded when almost 65% of control roots were 5 mm long (USEPA, 1996). Soybean seedlings were rinsed first with 0.01M HNO_3, then twice with MPW to eliminate any surface metal. Percent germination, relative germination, germination change, and the size of 10 roots plus hypocotyls were determined.

Quantification of Zn and Ce in dry plant tissues

Samples were digested in a microwave acceleration reaction system (CEM Corp.; Mathews, NC) following the USEPA 3051 method using 3 mL of plasma pure HNO_3 for samples from ZnO NP treatments. The CeO_2 NP treated samples were digested with plasma pure HNO_3 and H_2O_2 (1:4) as described by Packer et al. (13), with slight modifications. Blank, spikes, and 1570a standard reference material (spinach leaves) were used to validate the digestion and analytical method for Zn. In addition, 0.05 ppm Ce and Zn standard were analyzed after every 10 samples for QC/QA purposes. Ten blanks were analyzed in order to calculate the detection limit for Zn and Ce.

Genomic DNA Isolation

For DNA isolation, seeds were treated with 2000 and 4000 mg L^{-1} of either ZnO or CeO_2 NPs. Control seeds were germinated with MPW. After 1 week, 9 root tips were treated with the Wizard™ Genomic DNA extraction kit (Promega A1120). DNA yield was determined using the Nanodrop spectrophotometer for quantification of double stranded DNA.

RAPD procedures

Polymerase chain reactions were performed in 25μL reaction mixtures containing 12.5μL of Green GoTaq® Green Master Mix. GoTaq® DNA Polymerase is supplied in 2X Green GoTaq® Reaction Buffer (pH 8.5), 400μM dATP, 400μM dGTP, 400μM dCTP, 400μM dTTP, and 3mM $MgCl_2$ (Promega M7122). An aliquot of 2.5μL 10μM primer OPA03 (AGTCAGCCAC), and 20–50ng of genomic DNA were used for each PCR reaction from control and treated plants. Amplifications were performed in a Mycycler thermocycler system

(BioRad, Hercules, CA) programmed for 5 min denaturation at 95°C (initial denaturation); 40 consecutive cycles each consisted of 50s at 95°C (denaturing), 50s at 45.8°C (annealing), 1min at 72°C (extension), followed by 1 cycle for 7 min at 72°C. After amplification, RAPD reaction products were analyzed by electrophoresis on 1.6% agarose gels stained with ethidium bromide (1μg mL^{-1}) in 0.5X TBE (90mM Tris base, 90mM boric acid, and 2mM EDTA) buffer. The 100bp DNA ladder from Promega (G2101) was used as a molecular weight DNA standard. Gels were visualized and photographed under UV light on a Gel Doc XR system (BioRad, Hercules, CA, USA). The size of each amplification product was estimated using the Quantity One 4.6.8. band analysis feature.

RAPD profiles and data analysis

With the objective of investigating the genetic effect of ZnO and CeO_2 NPs on soybean seedlings, the RAPD analysis was performed using one random 10-mer. Reproducible amplification bands were scored for the construction of the data matrix. Only bands present in at least 70% of the 9 replicates were considered for the analysis. Changes in RAPD profiles were scored as present (1) and absent (0); changes in band intensities were not considered for the analysis. Genetic similarity coefficients among the roots of control and treated seedlings were estimated from Nei's unbiased measure (14) in POPGENE version 1.31. Cluster analysis was performed and a dendrogram was generated using the unweighted pair group method with the arithmetic means (UPGMA) algorithm of POPGENE 1.31.

Sample preparation for XAS studies

Roots of soybean seedlings exposed to 4000 mg of ZnO L^{-1} and CeO_2 L^{-1} were immersed in liquid nitrogen for 45 min and lyophilized on a freeze-dryer at −53°C and 0.140 mBar pressure for 3 days (Labconco FreeZone 4.5, Kansas City, MO). Samples were mortar homogenized, loaded in aluminum sample holders, and covered with Mylar© Tape.

X-ray absorption spectroscopy experiments (XAS)

XAS spectra were collected on beam Line 7-3 at the Stanford Synchrotron Radiation Laboratory (SSRL, Palo Alto, CA). During data collection, the synchrotron radiation accelerator had ring storage energy of 3 GeV and a beam current of 50–100 mA. Zn-K edge and CeL_{III} spectra were collected using a Canberra 29-element germanium detector and Si (220) φ 90 monochromator. Zinc and cerium foils were used to calibrate sample spectra. Fluorescence and transmission mode were used for collecting all sample spectra and model compounds, respectively, at room temperature. Zinc nitrate, zinc acetate, ZnO NPs, as well as cerium nitrate and CeO_2 NPs were used as model compounds.

The WinXAS software (15) was used to analyze data. Edge energies from individual spectra were calibrated using the edge energy from the internal zinc or cerium foil (9659 and 5723 eV, respectively). First and second degree derivatives of the inflection point of the metal foil were used to calibrate the sample spectrum, and a polynomial fitting subtraction was done in order to remove background. A 1^{st} and 4^{th} degree polynomial were used on the pre-edge and post-edge region of the spectrum, respectively. Speciation of Zn and Ce was determined based on the X-ray absorption near edge structure (XANES) spectra from model compounds.

Statistical analysis

Treatments were arranged in a completely random design. Data were reported as mean ± standard error (SE) and SPSS 15.0 package was used to perform the one-way ANOVA and Tukey's H.S.D. test.

Results and Discussion

Effect of ZnO and CeO_2 NP on seed germination

In the present research, soybean seeds were treated either with hexagonal ZnO NPs (8 nm) or cubic CeO_2 NPs (7 nm) at 0, 500, 1000, 2000, and 4000 mg L^{-1}. ICP analyses indicated a purity of 100.0 % ± 3.0 for ZnO NPs and 98.0% ± 0.2 for CeO_2 NPs. Characterization from the XRD is shown in Figure 1 SI. The solid line in Fig. 1 (a) SI represents the XRD pattern from the CeO_2 nanoparticle ensemble. The data was indexed using the known lattice parameter (a=5.412Å) and spacegroup (Fm-3m) of the cubic CeO_2 unit cell. The Bragg reflection 2θ positions (vertical bars in Fig. 1 (a) SI), calculated according to the above-mentioned unit cell demonstrate the high purity of the CeO_2 nanoparticle ensemble (i.e no unindexed reflection are present in the observed XRD data). On the other hand, as Fig. 2 (b) SI shows, the indexing of the XRD pattern from the ZnO nanoparticle ensemble (solid line) to the tetragonal ZnO phase - lattice parameter (a=3.249Å, c=4.206Å) and spacegroup ($P6_3mc$) – leaves at least two Bragg peaks unindexed. This indicates that an impurity phase is present in the sample.

Seedlings were harvested after 5 days of germination. Except for the 2000 mg CeO_2 L^{-1} treatment, none of the NP treatments significantly reduced soybean germination (Figure 2, SI). Lin and Xing (6) reported that 2000 mg ZnO NPs L^{-1} (20 nm) inhibited corn germination but did not affect the germination of radish, rape, ryegrass, lettuce, and cucumber. This suggests that the toxicity of ZnO NPs is species specific and also size dependent. As for CeO_2 NPs, to the authors' knowledge no other reports exist pertaining to their effects on seed germination.

Effect of ZnO and CeO_2 NP on biomass production and root growth

ZnO and CeO_2 NPs differentially affected root elongation (Figure 1). All the CeO_2 concentrations significantly increased root elongation. At 4000 mg L^{-1}, the root size was increased by 75%, ($p \leq 0.05$), compared to controls (Figure 1, bottom). Conversely, an inverse U-shape response was observed in ZnO NP treated seedlings, with maximum size at 500 mg L^{-1} (30% over control) and a minimum at 4000 mg L^{-1} (40% shorter than control), ($p \leq 0.05$). These results were in agreement with those found by Lin and Xing (6), who reported a significant decrease in root growth when several plant species were exposed to 2000 mg L^{-1} ZnO NP.

Zn is an essential element for plant growth and development. A great number of proteins contain a Zn-binding domain, such as transcriptional regulatory proteins (16). However, above certain concentrations this element becomes toxic, causing plants to activate different defense mechanisms such as the increase in the expression of lignin and suberin biosynthesis genes (17). Lignification has also been reported in other plants treated with zinc, including *Zea mays* (18). The effects of ZnO NPs on soybean germination and root elongation may be due to the NPs per se and the zinc ions resulting from ZnO dissolution.

Cerium belongs to the lanthanide elements. Some of these elements have been used for agricultural purposes due to their beneficial effect on plant resistance and development (19, 20). For example, La(III) reduces UV-B damage in soybean chloroplasts (21) and Ce(III) regulates photosynthesis under UV-B irradiation (20). Peach seedlings treated with $CeCl_3$ increased root weight and root length (22). However, the effect of CeO_2 NPs on plant development or its biotransformation has not been reported. The XAS data (Figure 3) showed that Ce in CeO_2 NPs has an oxidation state of (IV); unfortunately, to our knowledge, no data has been reported on the effect of Ce(IV) in plants. Thus, careful comparisons with data obtained from Ce(III) should be made, but this result may still serve as a reference.

Zinc and Ce uptake by soybean

The ICP-OEs result from the certified reference material for Zinc showed a recovery of 99%; which validates the results of this study. The uptake of Zn and Ce by soybean seedlings proved to be quite different (Figure 2). The highest Zn accumulation was obtained at 500 mg L^{-1} of ZnO NPs (229 mg Zn kg^{-1} DW). While at 1000, 2000, and 4000 mg L^{-1} treatments, plant Zn concentrations varied from 135 to 150 mg Zn kg^{-1} DW (Figure 2, upper). As previously reported (23), Zn uptake can be driven by the agglomeration of the NPs in the media as well as NP dissolution. Franklin et al.(23) reported that ZnO at 100 mg/L showed a agglomeration resulting in flocs formations from different sizes (nm to μm). The data suggest that at 500 mg L^{-1} the agglomeration was lower than at 4000 mg L^{-1}, resulting in more NPs and Zn ions available for plant uptake.

Figure 2 also shows the Ce concentrations in soybean tissues. As seen in the figure, Ce in tissues increased as external concentration of CeO_2 NPs increased. Seedlings exposed to 4000 mg L^{-1} had 462 mg Ce kg^{-1} DW, which was about 3-fold the amount of Zn (153 mg kg^{-1} DW) found in seedlings treated with 4000 mg L^{-1} ZnO NPs. The ICP-OES data showed that Ce concentration in the supernatant of the 4000 mg CeO_2 NPs L^{-1} suspension, the same day of the experimental set up, was below the detection limit (0.048 mg Ce L^{-1} and 0.018 mg Zn L^{-1}). These results are in agreement with those reported by Hoecke et al. (25), who found that the amount of Ce dissolved from 50 mg L^{-1} of CeO_2 NP suspension was insignificant. Moreover, the concentration of Zn found in the supernatant of the 4000 mg ZnO NPs L^{-1} was 8.0 ± 0.2 mg L^{-1}. This suggests that the CeO_2 NPs are more easily absorbed by soybean plants than ZnO NPs. In addition, in the present study, the XAS analysis (Figure 3) showed no modification of CeO_2 NPs within soybean seedlings. However, in other organisms like *Escherichia coli*, CeO_2 NPs were absorbed and modified significantly onto the membrane (24).

Speciation of Zn and Ce in root tissues

As seen in Figure 3, a distinctive double white line feature at 5.730 and 5.737 KeV is present in the spectrum of CeO_2 NPs (used as model compound), corresponding to a typical mixture of two ground-state electronic configurations of Ce ($4f^0$ and $4f^1$) (26). In addition, CeN_3O_9 was also used as model compound revealing the oxidation state of (III). The CeL_{III}- edge normalized XANES spectrum revealed that soybean roots uptake and store CeO_2 NPs. Ce was found in the same oxidation state (IV) inside roots, as in the CeO_2 NPs. To the best of the authors' knowledge, this is the first report on the presence of CeO_2 NPs in the roots of higher plants, using XAS technique. Hoecke et al. (25) reported the toxicity effects of three sizes of CeO_2 NP on *Pseudokirchneriella subcapitata*, *Daphnia magna* and *Thamnocephalus platyurus*, and *Danio rerio*. These researchers reported a differential response to NP toxicity in aquatic organisms from varied trophic levels. Some of the parameters studied by these researchers were growth inhibition, reproduction, and mortality. They found that chronic toxicity was greater from smaller CeO_2 NPs; however, they did not determine the form of CeO_2 NP within tissues.

Figure 4 shows the XANES spectra from the K-edge energy for Zn (E_0= 9659 eV). ZnO NP powder, Zn-acetate, and Zn-nitrate were used as model compounds. The XANES spectra from roots treated with 4000 mg ZnO NP L^{-1} showed that within tissues Zn was in the oxidation state of Zn(II) but not present as ZnO NPs. Zn appeared coordinated in the same manner as Zn-nitrate or Zn-acetate (Figure 4). Reports indicate that within plants Zn has been found as Zn-hydroxides and Zn^{+2} (27). Another report suggested the presence of ZnO NPs, based on TEM micrographs of ryegrass cross sections (*Lolium perenne*) (6); however, analytical evidence of this assumption was not provided.

RAPD results

Higher plants such as soybean can be used as bioindicators for nanotoxicity. An essential area of study is genotoxicology, the study of genetic aberrations following exposure to NPs. A few genotoxic studies have been performed on mammalian and human cell lines; however, reports on plants are scarce (28). Effects of genotoxins have been studied using chromosome aberrations, micronucleus, and comet assays (29). An alternative new approach is the use of the RAPD assay. RAPD can potentially detect a wide range of DNA damage and mutations; it can therefore be applied to study NPs genotoxicity (30). In this study, the total number of representative bands identified in the control was 8 and ranged from 300 to 1600 bp. A total of 14 bands were detected (appearing and disappearing bands in all control and treated plants) using the band analysis feature of quantity one. Figure 5 shows the RAPD profiles for all treatments and Table 1 shows the data matrix used for the genetic identity analysis. The RAPD profile from roots treated with ZnO at 2000 mg L^{-1} was similar to the one of control plants. However, at 4000 mg L^{-1}, a new band of 519 bp appeared in the profile. Unfortunately, there are no previous reports pertaining to plants. However, in other living systems such as Chinese hamster ovary (CHO) cells, Dufuor et al. (31) demonstrated the genotoxic effects of ZnO nanoparticles (100 nm diameter) using the chromosome aberration test. The lowest concentration that was tested (54 mg L^{-1}) produced a significant increase in DNA damage. Moreover, the authors demonstrated an enhancement of ZnO NP genotoxicity by UV exposure. Zn is an important cellular nutrient and ZnO NPs are considered biocompatible; however, the results of the present study demonstrated that ZnO NPs could have an impact on the genetic material of terrestrial plants. The presence of new bands may reveal a change in the priming sites leading to new annealing events. Also, large deletions and homologous recombination could lead to the appearance of new bands (30). Zn ions released from NPs can convert cellular oxygen metabolic products such as H_2O_2 and superoxide anions into hydroxyl radicals, a primary DNA damaging species (28). Through this mechanism, ZnO NPs could be affecting the genetic stability of soybean plants. Therefore, it is important to investigate the amount of Zn that could be leaching out of the NPs in order to confirm if the observed genotoxicity was due to the released Zn ions, or rather, was a direct interaction of the NPs with the DNA.

The exposure of soybean plants to CeO_2 NPs produced four new bands at 2000 mg L^{-1} and three at 4000 mg L^{-1} treatments. This result demonstrated the genotoxicity of CeO_2 NPs on soybean plants. Previous reports from toxicological studies of CeO_2 NPs in animal cells are controversial. Schubert et al. (32) demonstrated a ROS protective effect in HT22 cells derived from rodent nervous systems. The antioxidant effect of CeO_2 NPs was independent of the size (6 nm, 12 nm, and 1 μm) but dependant of the concentration (from 0.0002 to 20 mg L^{-1}). On the other hand, Park et al. (33) reported induced oxidative stress by CeO_2 NPs in cultured human lung epithelial cells (BEAS-2B). It is well known that increasing oxidative stress leads to DNA damage that affects RAPD profiles. This could cause the appearance of the new bands in soybean plants. Park et al. (33) also found an increase in chromatin condensation in human lung cells treated with 30 nm CeO_2 NPs. The dual oxidation state (III and IV) of CeO_2 NPs is responsible for the interesting redox chemistry exhibited by these NPs (34). However, the ratio of Ce(III) to Ce(IV) ions in the NP surface depends on the size and preparation method of the NPs. Oxidative stress induced on BEAS-2B cells and the effect observed in soybean roots exposed to CeO_2 NPs may be due to the lack of enough Ce^{+3} ionic state to scavenge oxygen radicals leading to oxidative DNA damage.

Figure 3 (Supporting information) shows a dendrogram constructed based on UPGMA analysis of RAPD data. In the present study, the estimated Nei genetic identity coefficient (NGI, from Table 1) for 2000 mg ZnO L^{-1}, 2000 mg CeO L^{-1}, and 4000 mg CeO L^{-1} were found to be lower compared to controls NGI value is 1.00 for control treatments. Cluster analysis revealed two main groups: one composed of control and ZnO treated plants, and the other formed by

CeO_2 treated plants. RAPD has shown that both ZnO and CeO_2 NPs do affect the integrity of the DNA, but CeO_2 NPs caused the highest effect on the genetic stability of soybean plants.

Supplementary Material

Refer to Web version on PubMed Central for supplementary material.

Acknowledgments

This material is based upon work supported by the National Science Foundation and the Environmental Protection Agency under Cooperative Agreement Number EF 0830117. Any opinions, findings, conclusions or recommendations expressed in this material are those of the author(s) and do not necessarily reflect the views of the National Science Foundation or the Environmental Protection Agency. This work has not been subjected to EPA review and no official endorsement should be inferred. Portions of this research were carried out at the Stanford Synchrotron Radiation Laboratory, a national user facility operated by Stanford University on behalf of the U.S. Department of Energy, Office of Basic Energy Sciences. The SSRL Structural Molecular Biology Program is supported by the Department of Energy, Office of Biological and Environmental Research, and by the National Institutes of Health, National Center for Research Resources, Biomedical Technology Program. J.L. Gardea-Torresdey acknowledges the USDA grant # 2008-38422-19138, the LERR and STARs programs of the UT System, the Dudley family for the Endowed Research Professorship in Chemistry, the Toxicology Unit of the BBRC (NIH NCRR Grant # 2G12RR008124-16A1) and the NSF Grant # CHE-0840525. G. de la Rosa acknowledges the Mexican National Council for Science and Technology CONACYT (CB 61649), and the Council for Science and Technology in Guanajuato (08-16-k662-127)

References

1. Kasthuri J, Veerapandian S, Rajendiran N. Biological synthesis of silver and gold nanoparticles using apiin as reducing agent. Colloid Surface B 2009;68:55–60.
2. Darlington TK, Neigh AM, Spencer MT, Nguyen OT, Oldenburg SJ. Nanoparticle characteristics affecting environmental fate and transport through soil. Environ. Toxicol. Chem 2009;28:1191–1199. [PubMed: 19175296]
3. Pidgeon N, Harthorn BH, Bryant K, Rogers-Hayden T. Deliberating the risks of nanotechnologies for energy and health applications in the United States and United Kingdom. Nature Nanotech 2009;4:95–98.
4. Castillo-Michel H, Valente N, Martinez-Martinez A, Parsons JG, Peralta-Videa JR, Gardea-Torresdey JL. Coordination and speciation of cadmium in corn seedlings and its effects on macro-and micronutrients uptake. Plant Physiol. Biochem 2009;47:608–614. [PubMed: 19285423]
5. Yap CK, Chua BH, Teh CH, Tan SG, Ismail A. Patterns of RAPD markers and heavy metal concentrations in *Perna viridis* (L.), collected from metal-contaminated and uncontaminated coastal waters: Are they correlated with each other? Russ. J. Genet 2007;43(5):544–550.
6. Lin D, Xing B. Phytotoxicity of nanoparticles: inhibition of seed germination and root growth. Environ. Pollut 2007;150:243–250. [PubMed: 17374428]
7. Czernichowski A, Czernichowski M, Wesolowska K. Generation of 1 kg/h of hydrogen from soybean biodiesel. Preprints of Symposia: ACS, Division of Fuel Chemistry 2006;51:619–620.
8. Murakami M, Ae N, Ishikawa S. Phytoextraction of cadmium by rice (*Oryza sativa* L.), soybean (*Glycine max* (L.) Merr.), and maize (*Zea mays* L.). Environ. Pollut 2007;145:96–103. [PubMed: 16781805]
9. Maejima Y, Makino T, Takano H, Kamiya T, Sekiya N, Itou T. Remediation of cadmium-contaminated paddy soils by washing with chemicals: Effect of soil washing on cadmium uptake by soybean. Chemosphere 2007;67:748–754. [PubMed: 17141294]
10. Bernal M, Cases R, Picorel R, Yruela I. Foliar and root Cu supply affect differently Fe- and Zn- uptake and photosynthetic activity in soybean plants. Environ. Exp. Bot 2007;60:145–150.
11. Barrena R, Casals E, Colón J, Font X, Sánchez A, Puntes V. Evaluation of the ecotoxicity of model nanoparticles. Chemosphere 2009;75:850–857. [PubMed: 19264345]
12. Culity, BD. Elements of X-ray Diffraction. 2nd Ed.. New York: Addison-Wesley; 1978. p. 101-102.
13. Packer AP, Lariviere D, Li C, Chen M, Fawcett A, Nielsen K, Mattson K, Chatt A, Scriver C, Erhardt LS. Validation of an inductively coupled plasma mass spectrometry (ICP-MS) method for the

determination of cerium, strontium, and titanium in ceramic materials used in radiological dispersal devices (RDDs). Anal. Chim. Acta 2007;588:166–172. [PubMed: 17386806]

14. Nei M. Estimation of average heterozygosity and genetic distance from a small number of individuals. Genetics 1978;89:583–590. [PubMed: 17248844]
15. Ressler T. WinXAS: a program for X-ray absorption spectroscopy data analysis under MS-Windows. J. Synchrotron Radiat 1998;5:118–122. [PubMed: 16687813]
16. Kochian, LV. Molecular physiology of mineral nutrient acquisition, transport, and utilization. In: Buchanan, B.; Gruissem, W.; Jones, R., editors. Biochemistry and Molecular biology of plants. Rockville, MD: American Society of Plant Physiologists; 2000. p. 1237-1239.
17. Van der Mortel JE, Villanueva LA, Schat H, Kwekkeboom J, Coughlan S, Moerland PD, van Themaat EVL, Koornneef M, Aarts MGM. Large expression differences in genes for iron and zinc homeostasis, stress response, and lignin biosynthesis distinguish roots of *Arabidopsis thaliana* and the related metal hyperaccumulator *Thlaspi caerulescens*. Plant Physiol 2006;142:1127–1147. [PubMed: 16998091]
18. Vieira da Cunha KP, Araujo do Nascimento CW, Pimentel RM de M, Accioly AM de A, da Silva AJ. Cadmium and zinc availability, accumulation and toxicity in maize grown in a contaminated soil. Rev. Bras. Cienc. Solo 2008;32-3:1319–1328.
19. An LZ, Wang XL. Effect of ozone on growth of spring wheat and the prevention of rare earth to ozone injury. Acta Ecol. Sinica 1994;14-1:95–98.
20. Lian CJ, Huang XH, Zhuo Q. Effect of cerium on photosynthetic characteristics of soybean seedling exposed to supplementary ultraviolet-B radiation. J. Environ. Sci 2006;18-6:1147–1151.
21. Peng Q, Zhou Q. Influence of lanthanum on chloroplast ultrastructure of soybean leaves under ultraviolet-B stress. J. Rare Earth 2009;27-2:304–307.
22. Weiping S, Fashui H, Zhigang W, Yuzhen Z, Fugen G, Hongoing X, Mingliang Y, Youhong C, Mizhen Z, Jiale S. Effects of cerium on nitrogen metabolism of peach plantlet in vitro. Biol. Trace Elem. Res 2003;95:259–268. [PubMed: 14665731]
23. Franklin NJ, Rogers SC, Apte GE, Batley GE, Gadd PS, Casey PS. Comparative toxicity of nanoparticulate ZnO, bulk ZnO, and $ZnCl_2$ to a freshwater microalga (*Pseudokirchneriella subcapitata*): The importance of the particle solubility. Environ. Sci. Technol 2007;41:8484–8490. [PubMed: 18200883]
24. Thill A, Zeyons O, Spalla O, Chauvat F, Rose J, Auffan M, Flank AM. Cytotoxicity of CeO_2 nanoparticles for *Escherichia coli*. Physico-chemical insight of the cytotoxicity mechanism. Environ. Sci. Technol 2006;40(19):6151–6156. [PubMed: 17051814]
25. Hoecke KV, Quik JTK, Mankiewicz-Boczek J, De Schamphelaere KAC, Elsaesser A, Van Der Meeren P, Barnes C, Mckerr, Howard CV, Van De Meent D, Rydzynski K, Dawson KA, Salvati A, lesniak A, Lynch I, Silversmit G, De Samber B, Vincze L, Janseen CR. Fate and effects of CeO_2 nanoparticles in aquatic ecotoxicity tests. Environ. Sci. Technol 2009;43:4537–4546. [PubMed: 19603674]
26. Shahin AM, Grandjean F, Long GJ, Schuman TP. Cerium L-edge XAS investigation of the structure of crystalline and amorphous cerium oxides. Chem. Mater 2005;17:315–321.
27. Auffan M, Rose J, Wiesner MR, Bottero JY. Chemical stability of metallic nanoparticles: A parameter controlling their potential cellular toxicity in vitro. Environ. Pollut 2009;157:1127–1133. [PubMed: 19013699]
28. Singh N, Manshian B, Jenkins GJ, Griffiths SM, Williams PM, Maffeis TG, Wright CJ, Doak SH. Nanogenotoxicology: The DNA damaging potential of engineered nanomaterials. Biomaterials 2009;30:3891–3914. [PubMed: 19427031]
29. Landsield R, Maike DK, Schulz M, Wiench K, Oesch F. Genotoxicity investigations on nanomaterials: Methods, preparation and characterization of test material, potential artifacts and limitations—Many questions, some answers. Mutat. Res 2009;681:241–258. [PubMed: 19041420]
30. Atienzar FA, Jha AN. The random amplified polymorphic DNA (RAPD) assay and related techniques applied to genotoxicity and carcinogenesis studies: A critical review. Mutat. Res 2006;613:76–102. [PubMed: 16979375]
31. Dufour EK, Kumaravel T, Nohynek GJ, Kirkland D, Toutain H. Clastogenicity, photo-clastogenicity or pseudo-photo-clastogenicity: genotoxic effects ofzinc oxide in the dark, in pre-irradiated or

simultaneously irradiated Chinese hamster ovary cells. Mutat. Res 2006;607:215–224. [PubMed: 16797222]

32. Schubert D, Dargusch R, Raitano J, Chan S. Cerium and yttrium oxide nanoparticles are neuroprotective. Biochem. Biophys. Res. Comm 2006;32:86–91. [PubMed: 16480682]
33. Park EJ, Choi J, Park YK, Park K. Oxidative stress induced by cerium oxide nanoparticles in cultured BEAS-2B cells. Toxicology 2008;245:90–100. [PubMed: 18243471]
34. Robinson RD, Spanier JE, Zhang F, Chan SW, Herman IP. Visible thermal emission from sub-band-gap laser excited cerium dioxide particles. J. App. Phys 2002;92:1936–1941.

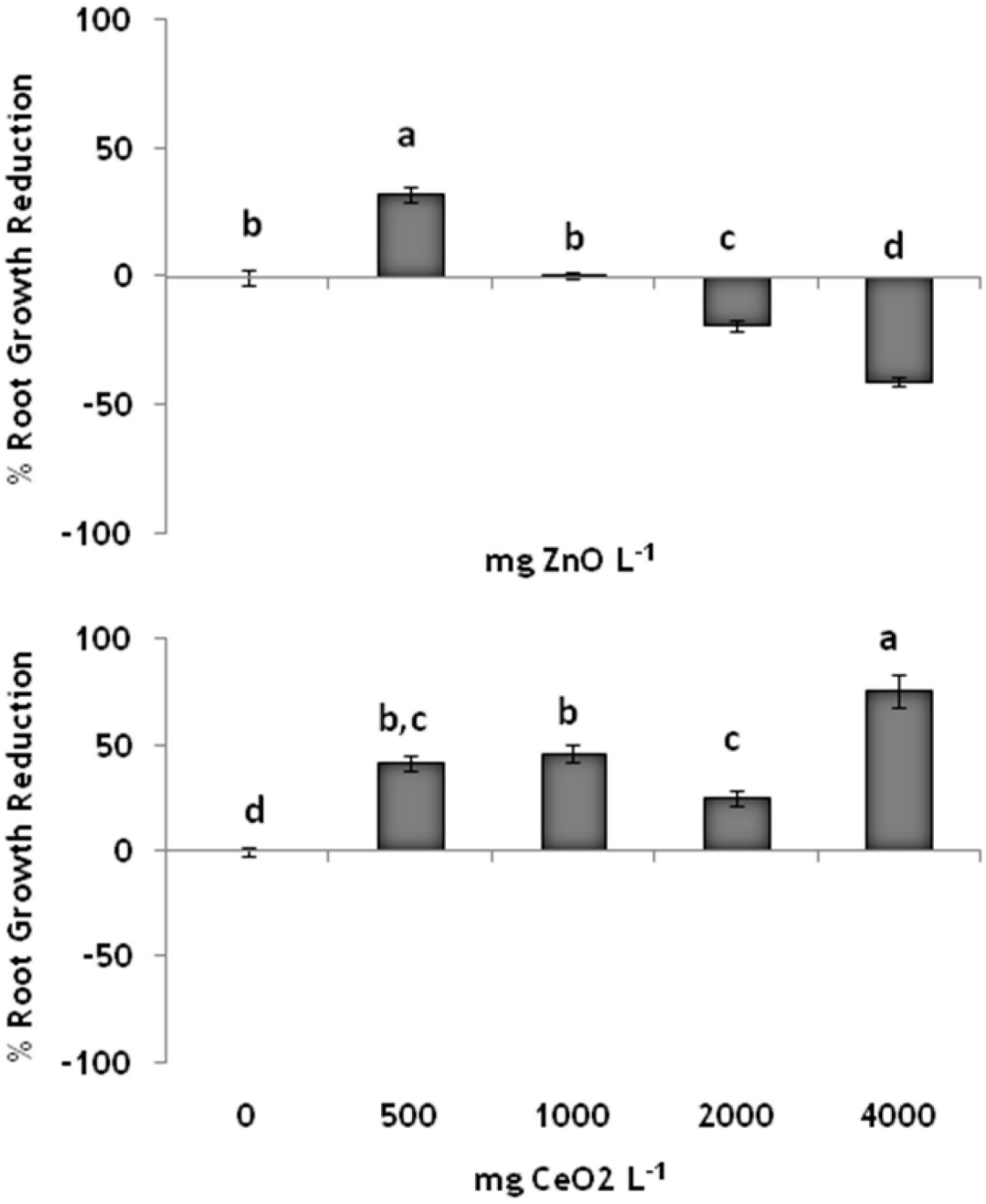

Figure 1.

Percent root growth reduction of soybean plants treated with 0–4000 mg/L ZnO and CeO_2 NPs. Data are means ± SE (standard error) of three replicates. Lowercases indicate statistically significant differences at $p < 0.05$.

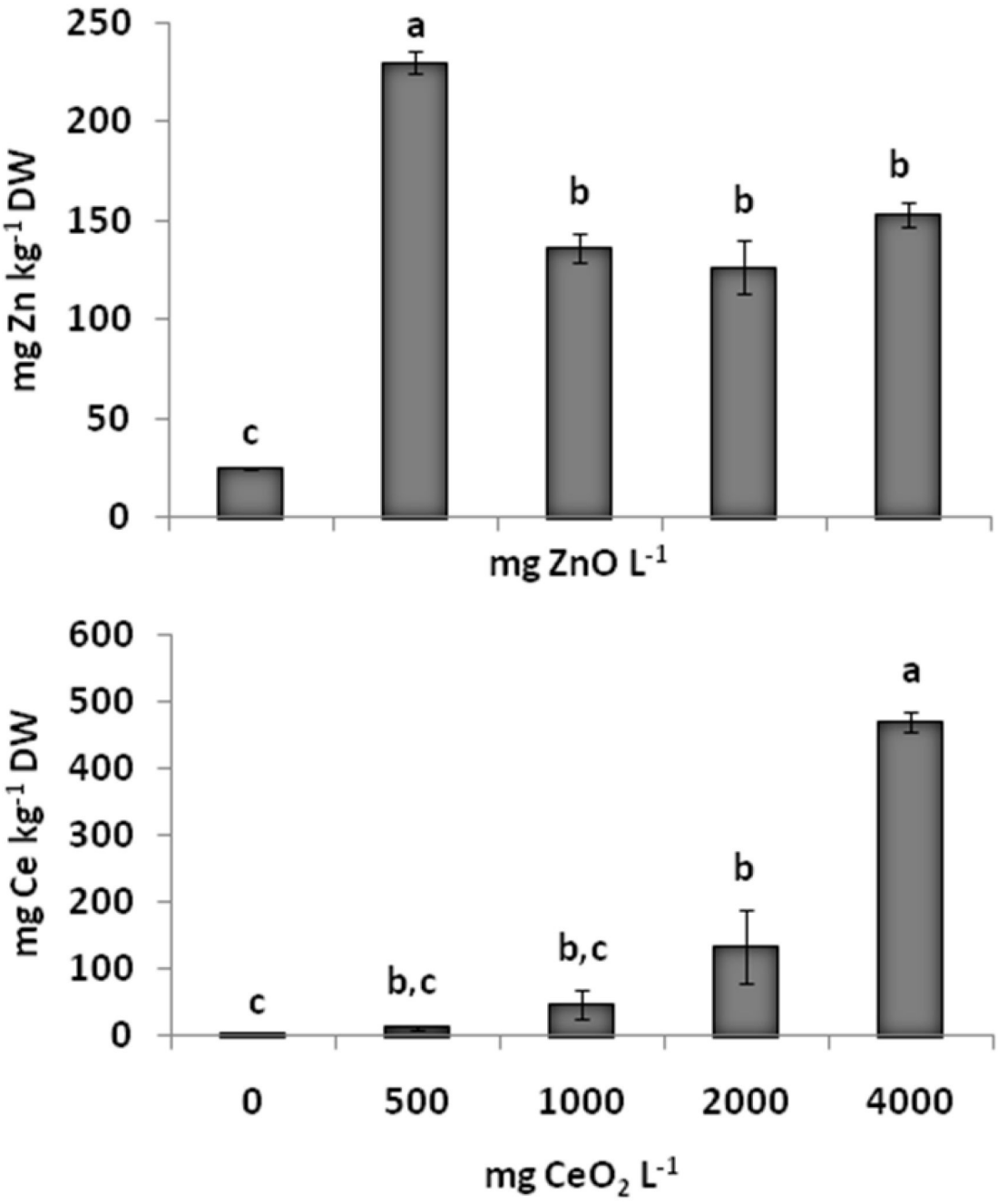

Figure 2.
Zinc and Ce concentration in soybean seedlings germinated in 0–4000 mg/L NP suspensions. Data are means of three replicates ± SE (standard error). Lowercase letters indicate statistically significant differences in Zn content in each plant species at $p \leq 0.05$.

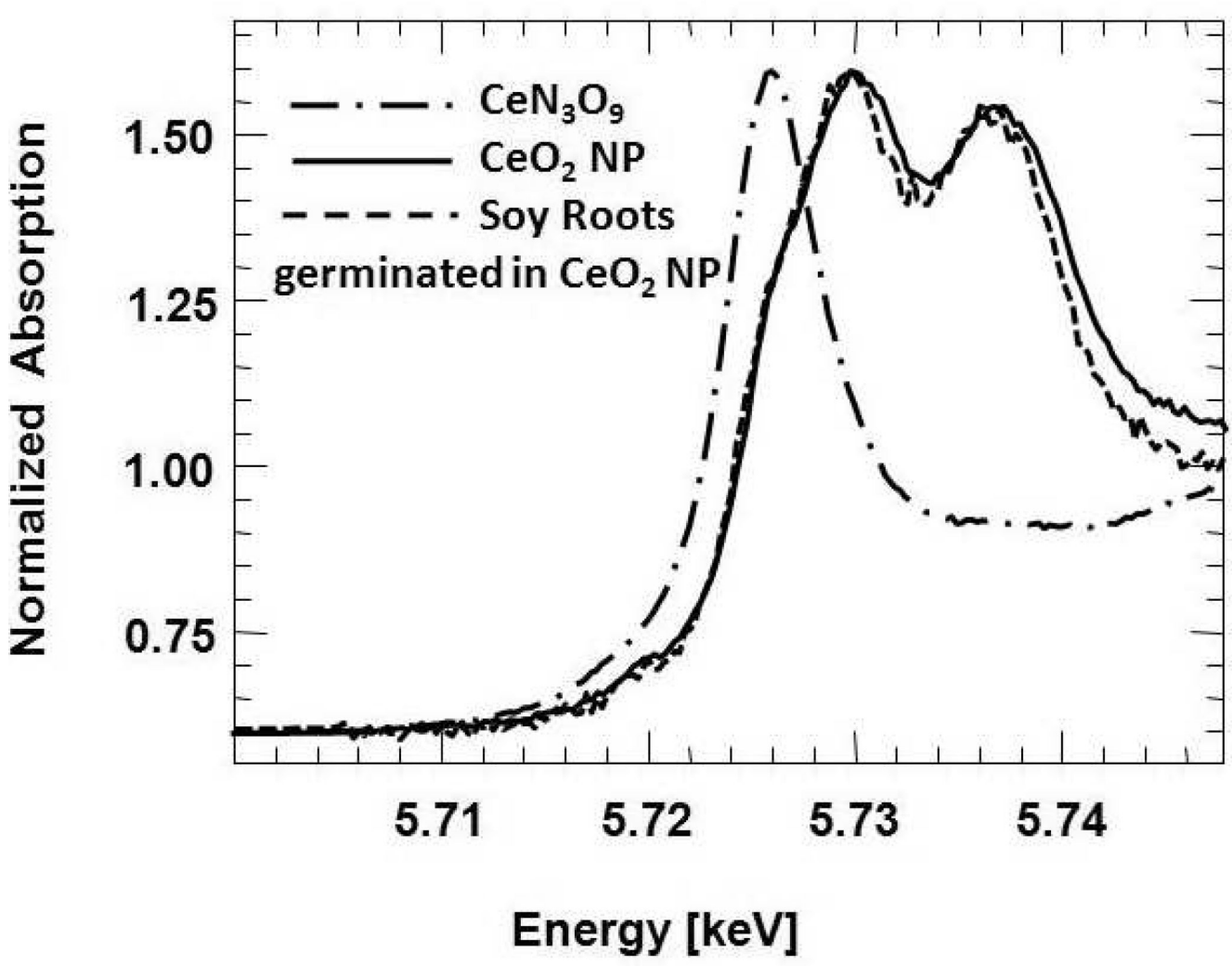

Figure 3.
XANES L_{III}-edge spectra (5723 eV) of CeO_2 NPs, CeN_3O_9 model compounds, and spectra from soybean roots germinated in 4000 mg/L of CeO_2 NPs.

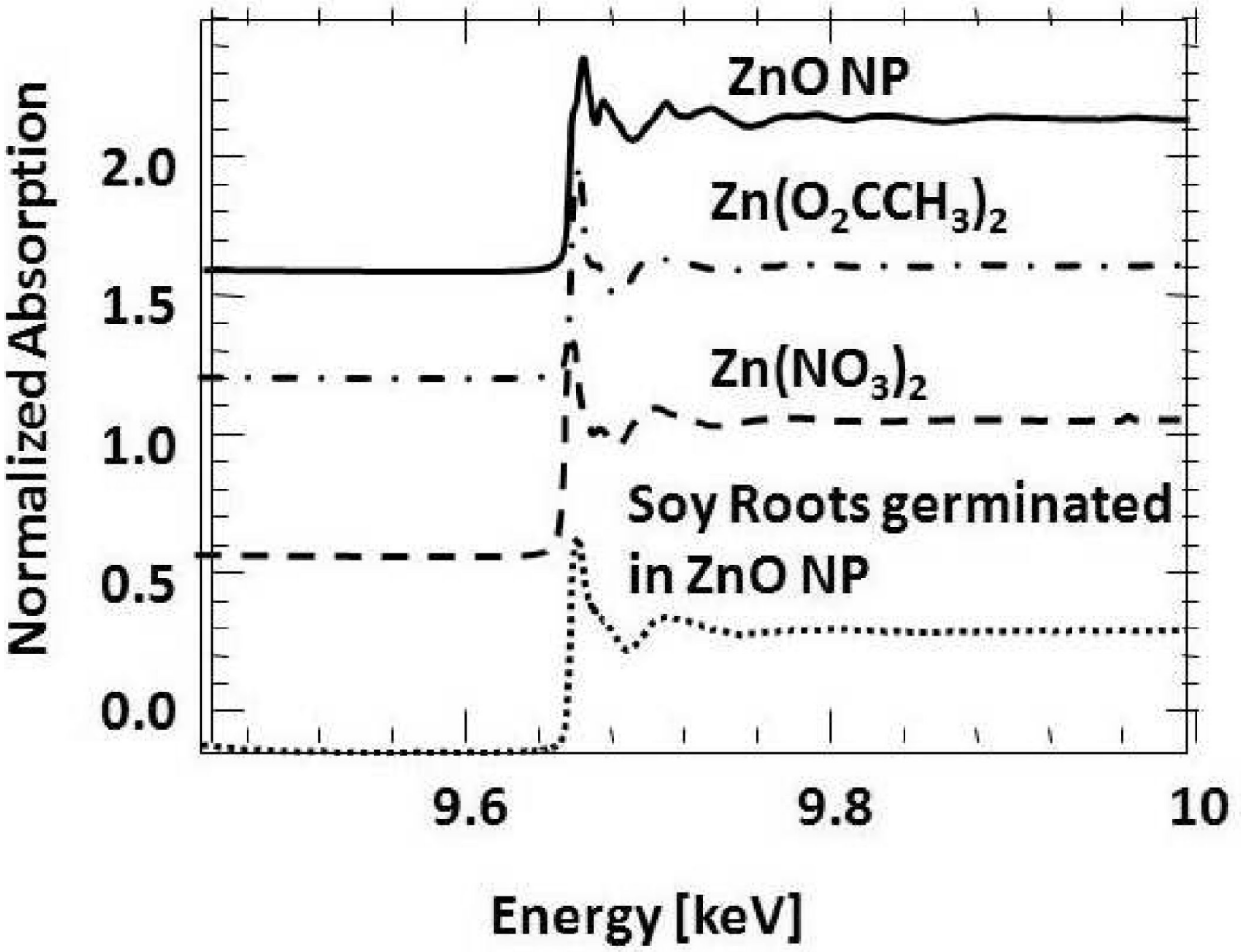

Figure 4.
XANES K-edge spectra (9659 eV) of ZnO NPs, Zn $(NO_3)_2$, and Zn $(O_2CCH_3)_2$ model compounds and spectra from soybean roots germinated in 4000 mg/L of ZnO NPs.

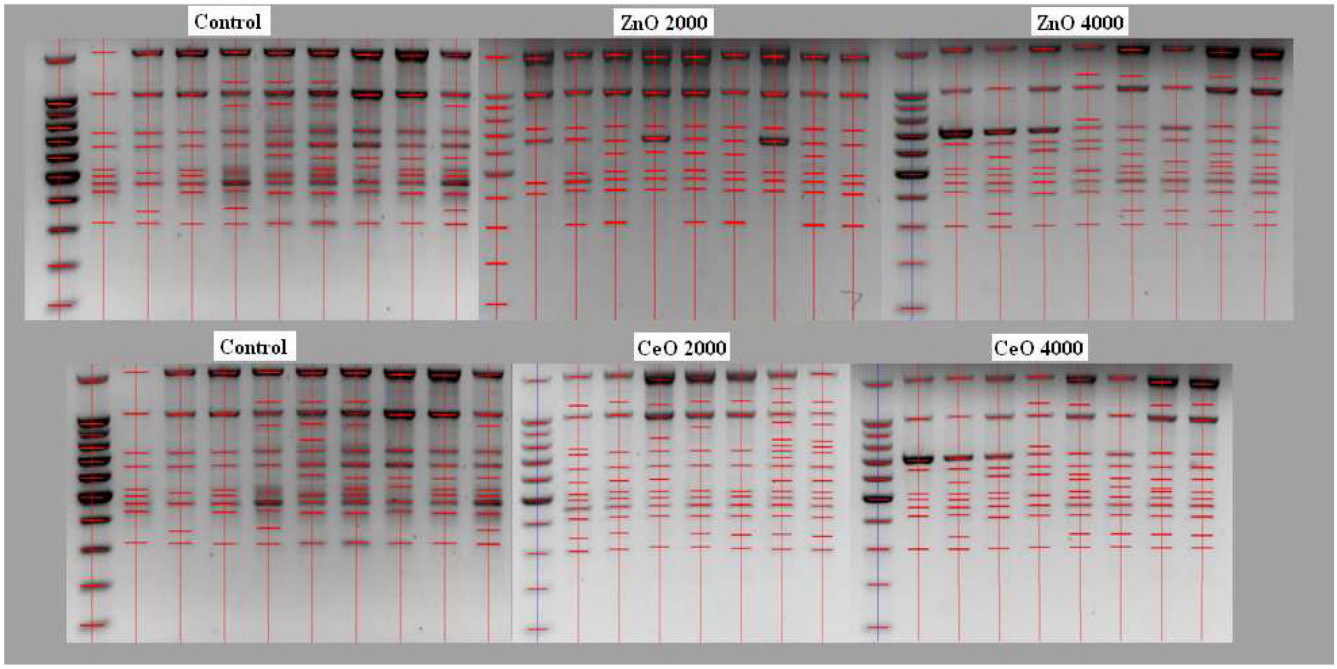

Figure 5.
RAPD profiles in the roots of soybean seedlings treated with ZnO and CeO_2 nanoparticles at 0 (control), 2000 mg L^{-1}, and 4000 mg L^{-1}. RAPD profiles were generated using primer OPA03. First lane in all gels is 100 bp DNA Ladder (100–1500 bp).

Table 1

Number and molecular size (base pair, bp) of bands detected in control, ZnO, and CeO_2 NP treated roots of soybean seedlings. (1) stands for present band (0) for absent bands for primer OPA03 (Gray box indicates appearing bands). Nei's genetic identity coefficient (NGI) was determined using the UPGMA method in Popgene 1.6.

	band size	control	ZnO 2000	ZnO 4000	CeO 2000	CeO 4000
1	1561	1	1	1	1	1
2	1216	0	0	0	1	0
3	1066	1	1	1	1	1
4	753	1	1	1	1	1
5	670	1	1	1	1	1
6	581	0	0	0	1	1
7	544	0	0	0	1	0
8	519	0	0	1	0	0
9	505	1	1	1	1	1
10	468	1	1	1	1	1
11	439	1	1	1	1	1
12	411	0	0	0	0	1
13	353	0	0	0	1	1
14	309	1	1	1	1	1
	NGI	1.00	1.00	0.93	0.71	0.79